Conformational Studies of Substituted Five-membered Cyclic Carbonates and Related Compounds by MNDO, and the *X*-Ray Crystal Structure of 4-Chlorophenyloxymethyl-1,3-dioxolan-2-one

Jehoshua Katzhendler,[a] **Israel Ringel,**[b] **Amiram Goldblum,**[a] **Dan Gibson,**[a] **Zeev Tashma**[a]
Departments of Pharmaceutical Chemistry[a] *and Pharmacology*[b] *School of Pharmacy, The Hebrew University of Jerusalem, Israel*

Geometries, torsional barriers, and dipole moments have been computed for mono-, di-, tri-, and tetra-substituted five-membered cyclic carbonates and for some substituted cyclopentanones, oxolanes, 4-butyrolactones, and 1,3-dioxolanes. With respect to cyclic carbonates it was deduced that the potential curve increases moderately with T_{3456} (torsion angle) and for most compounds a 1 kcal difference between $^4T_5$ or $^5T_4$ conformers and planar form corresponds to a torsional angle of $\pm$14–16°. The minimum is, in general, flattened and close to planar. Additional modes of ring puckering such as ^5E, E_5, ^4E, E_4 and ^2E, E_2 were also examined. Between the enantiomeric structures with opposite distortions, the quasi equatorial conformation of the alkyl group is preferred.

endo and *exo* anomeric effects in carbonate systems have been studied by introducing strong electron-withdrawing substituents, in the carbonate 4-position. The *exo* anomeric effect was observed with many of the polar substituents, but the role of the anomeric effect in ring puckering (*endo* effect) was found to be small.

For other five-membered ring systems MNDO predicts that the energy barrier to interconversion of planar $\longleftrightarrow$ twist is in the following order: carbonates > 1,3-dioxolanes > butyrolactones > oxolanes > cyclopentanones.

N.m.r data are also included as well as the single-crystal *X*-ray diffraction study of 4-chlorophenyloxymethyl-1,3-dioxolan-2-one.

It is well documented and widely accepted that five-membered ring systems and cyclopentane exist in a continuous pseudorotation[1,2] mobility between 20 isoenergetic extreme conformations C_s (envelope or bent) and C_5 (half chair or twisted). The presence of substituents, or the inclusion of endocyclic or exocyclic heteroatoms in the ring is known to restrict the equilibrium by changing the torsion potential barriers of the pseudorotation circuit.[1d,3–7] It was predicted[1c] that substituents which increase the torsional barrier around the C–C bond favoured a C_s conformation while C_2 is preferred in cases of decreased rotational barriers. Thus, methyl substitution favours C_s conformation[1d,8,9] (with an inversion barrier of ~0.9 kcal mol^{-1})† while cyclopentanone has been shown to prefer the C_2 conformation.[1d,10,11] Oxolane[2d,10] and 1,3-dioxolane[10] were also predicted to restrict the pseudorotational motion while preferring the C_2 conformation. 2-Oxo-1,3-dioxolane, exists in the crystal[12] form in a half-chair conformation with the torsional angle O–C(4)–C(5)–O being 31°. N.m.r. data based on ^{1}H and ^{13}C chemical shifts and ^{1}H vicinal coupling constants are also in accord with this view.[13] On the other hand some of the results indicate a non-planar (C_{2v} symmetry) structure for ethylene carbonate.

In order to gain further insight into the conformational changes in the 2-oxo-1,3-dioxolane ring (ethylene carbonate), we have studied some substituted ethylene carbonates and iminocarbonates by n.m.r. spectroscopy, single-crystal *X*-ray diffraction studies and semiempirical MNDO calculations. The structure of the compounds studied is given in Table 1.

For comparison we also studied the conformational modes of some substituted cyclopentanone, oxolanes, 4-butyrolactones, and 1,3-dioxolanes (Table 2).

Results and Discussion

^{13}C *N.M.R. Long-range Coupling*.—The generally accepted approaches to conformational analysis by n.m.r. spectroscopy consist of ^{1}H and ^{13}C chemical shifts, vicinal (*R* values) and long range (^3J) coupling, and anisotropic effects of the substituents. Some of these methods have been used in the past for conformational assignment of the 2-oxodioxolane ring. The results strongly support the existence of a non-planar structure. The ^3J coupling between the protons on C-4 (or C-5) of the carbonate ring with ^{13}C=O (^{1}H–C–O–^{13}C=O) can also contribute to the evaluation of ring conformation.

Substituents on the carbonate ring might change the torsional angles and thus affect the ^3J coupling constant. Table 3 displays the long range coupling constants of ethylene carbonate derivatives; ^3J = 3.1 Hz for ethylene carbonate, is a time-averaged value of rapidly interconverting conformers. The *meso*-4,5-dimethyl isomer *c*-(**2c**) exhibits a ^3J value of 2.9 Hz which is similar to that of ethylene carbonate (digital resolution is *ca.* 0.2 Hz per point), so that a methyl substituent does not change the ^3J value.

The spectrum of ^{13}C=O coupled by the ring protons of *t*-4,5-dimethylethylene carbonate [*t*-(**2a**)] appears as a triplet with ^3J = 2.2 Hz. This low value can be attributed mainly to the changes in the torsional angles, probably due to a quasiequatorial and quasiaxial orientation of the methyl groups and ring hydrogens, respectively.

The coupled ^{13}C=O spectrum of 4-methylethylene carbonate displays two triplet signals (Figure 1) with ^3J values of 2.7 and

---

† 1 cal = 4.184 J.

Table 1. Notation of substituents in 2-oxo-1,3-dioxolanes[a] and 2-phenylimino-1,3-dioxolanes.

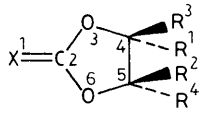

(b)

Compd.	X	R^1	R^2	R^3	R^4
(1)	O	H	H	H	H
(1a)	O	Me	H	H	H
(1b)	O	OMe	H	H	H
(1c)	O	Cl	H	H	H
(1d)	O	CH_2OMe	H	H	H
(1e)	O	CH_2Cl	H	H	H
(1f)	O	CH_2NMe	H	H	H
(1g)	O	Ph	H	H	H
(1h)	O	$CH_2OC_6H_4Cl$-*p*	H	H	H
(1i)	O	CH_2OCF_3	H	H	H
(1j)	O	OCF_3	H	H	H
(1k)	O	CH_2F	H	H	H
(1l)	O	$CH_2\overset{+}{N}Me_3$	H	H	H
(1m)	O	$OCCl_3$	H	H	H
t-**(2a)**	O	Me	Me	H	H
t-**(2b)**	O	OMe	OMe	H	H
t-**(2c)**	O	Cl	Cl	H	H
t-**(2d)**	O	CF_3	CF_3	H	H
t-**(2e)**	O	CCl_3	CCl_3	H	H
t-**(2f)**	O	CHF_2	CHF_2	H	H
g-**(2a)**	O	Me	H	Me	H
g-**(2b)**	O	OMe	H	OMe	H
g-**(2c)**	O	Cl	H	Cl	H
g-**(2d)**	O	CF_3	H	CF_3	H
g-**(2e)**	O	CCl_3	H	CCl_3	H
c-**(2a)**	O	Me	H	H	Me
c-**(2b)**	O	OMe	H	H	OMe
c-**(2c)**	O	Cl	H	H	Cl
c-**(2d)**	O	CF_3	H	H	CF_3
c-**(2e)**	O	CCl_3	H	H	CCl_3
(3)	O	Me	Me	Me	H
(4)	O	Me	Me	Me	Me
z-**(1a)**	NPh	Me	H	H	H
E-**(1a)**	NPh	Me	H	H	H
Z-**(1g)**	NPh	Me	H	H	H

[a] **(1)**, **(2)**, **(3)**, and **(4)** denote mono-, di-, tri-, and tetra-substitution. The abbreviations *t*, *c*, and *g* correspond to *trans*, *cis*, and *gem* configuration. [b] We decided to adopt the above notation to represent the numbering scheme for all the different groups of heterocyclic compound irrespective of their systematic nomenclature (*i.e.* 1,3-dioxolane has the oxygen atoms at positions 3 and 6). [c] *Z* and *E* denote *Z* and *E* configurations.

3.4 Hz. These values indicate again a non-planar conformation of the ring skeleton.

Table 2. Notation of substituents in cyclopentanones, 1,3-dioxolanes, oxolanes, and 4-butyrolactones.

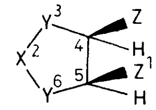

Compd.	X	Y^3	Y^6	Z	Z^1	R
(5)	C=O	CH_2	CH_2	H	H	—
(5a)	C=O	CH_2	CH_2	Me	H	—
(5b)	C=O	CHMe	CH_2	H	H	—
(6)	O	CH_2	CH_2	H	H	—
(6a)	O	CH_2	CH_2	Me	H	—
(6b)	O	CHMe	CH_2	H	H	—
(7)	CHR	O	O	H	H	H
(7a)	CHR	O	O	H	H	Me
(7b)	CHR	O	O	Me	H	H
(8)	C=O	O	CHR	H	H	H
(8a)	C=O	O	CHR	H	H	Me
(8b)	C=O	O	CHR	H	Me	H
(8c)	C=O	O	CHR	Me	H	H

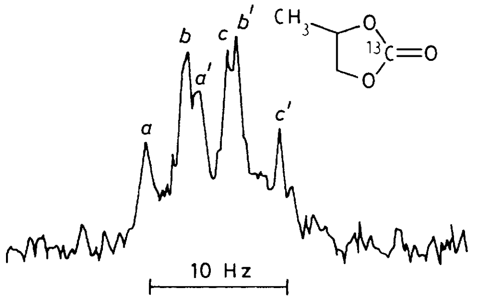

Figure 1. $^{13}C{=}O$ gated decoupling n.m.r. spectrum of **(1a)**.

MNDO Calculations.—In order to predict the preferred conformations of substituted 1,3-dioxolan-2-ones and of some other five-membered ring systems, MNDO semiempirical SCF calculations were carried out. All the geometrical parameters were fully optimized. Tables 4–6 summarize the theoretical bond lengths, bond angles, and torsion angles of the compounds in their optimized geometry. These tables present geometries and energy values which were calculated for the various compounds studied. Error estimates of quantum-mechanical values are dependent on the gradient convergence precision and are, in our calculations, about ± 0.0001 Å for bond lengths. However, the values for bond lengths and angles and values of enthalpies (precision of ± 0.0002 kcal mol^{-1}) must be compared with experiments which are less precise. Thus we present values of lower significance than the calculated precision. Table 4 presents the results for cyclopentanone, oxolane, 1,3-dioxolane, 4-butyrolactone, 2-oxo-1,3-dioxolane and for their monomethyl derivatives.

Cyclopentanone was calculated to be most stable in the planar conformation (Table 4). Its 2-methyl derivative **(5b)** is also planar, while 3-methylcyclopentanone **(5a)** has a discrete minimum in the C_2 form. In contrast with the reported data in the literature[10a,14] the calculated degree of puckering of the molecule is low (T_{3456} = 14.0° (T = torsional angle) compared with a reported value of 39–40°).

In the case of oxolanes, MNDO calculations predict a planar structure for the non-substituted compound and for its 2-methyl derivative, and a very small degree of puckering (T_{3456} = 4.3°) for the 3-methyloxolane. These results are inconsistent with pseudorotation assignments for furanose[15–17] rings and with previous[10a] quantum-mechanical data calculated for oxolane which indicate a preference for a C_2 conformation by 2.6 kcal over the planar form. Further MNDO calculations on 1,3-dioxolanes and 4-butyrolactones (Table 4) were in accord with a planar conformation. Although endocyclic or exocyclic hetero atom in a five-membered ring system imposes

Table 3. Coupling constants $^3J_{^1H-C-O-^{13}C=O}$ for five-membered cyclic carbonates (± 0.2 Hz).

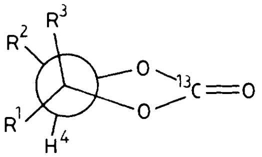

Compound		$^3J_{H(1),H(4)}$/Hz	$^3J_{H(2),H(3)}$/Hz	Multiplicity
(1)	$R_1 = R_2 = R_3 = H$	3.1	3.1	quintet
c-**(2a)**	$R_2 = R_3 = CH_3, R_1 = H$	2.9	2.9	t
t-**(2a)**	$R_1 = R_2 = CH_3, R_3 = H$	2.2	2.2	t
(1a)	$R_2 = CH_3, R_1 = R_3 = H$	2.7	3.4	dt

Table 4. Structural parameters of cyclopentanones, oxolanes, 1,3-dioxolanes, butyrolactones, and ethylene carbonates calculated by MNDO.

	(5)	**(6)**	**(7)**	**(8)**	**(1)**
	(5a)	**(6a)**	**(7a)**	**(8a)**	**(1a)**
	(5b)	**(6b)**	**(7b)**	**(8b)**	**(8c)**
$O-X^2$	1.222	—	—	1.219	1.217
	1.221	—	—	1.220	1.216
	1.221	—	—	1.220	1.220
X^2-Y^3	1.553	1.407	1.410	1.373	1.362
	1.553	1.405	1.415	1.372	1.369
	1.553	1.413	1.409	1.372	1.371
Y^3-C^4	1.540	1.552	1.406	1.412	1.420
	1.551	1.564	1.405	1.411	1.419
	1.538	1.550	1.412	1.411	1.418
C^1-C^5	1.545	1.539	1.561	1.557	1.629
	1.556	1.550	1.560	1.555	1.577
	1.549	1.539	1.572	1.569	1.567
C^5-Y^6	1.540	1.552	1.406	1.540	1.425
	1.540	1.551	1.405	1.551	1.412
	1.552	1.563	1.404	1.551	1.560
Y^6-X^2	1.534	1.407	1.410	1.534	1.363
	1.532	1.405	1.415	1.543	1.369
	1.544	1.406	1.409	1.533	1.532
$\angle 123$	124.99	—	—	118.35	124.75
	124.96	—	—	118.05	124.73
	124.40	—	—	118.36	118.29
$\angle 234$	106.67	108.34	111.85	112.17	112.44
	106.72	108.61	112.08	112.34	111.12
	106.72	108.39	112.50	112.31	112.64
$\angle 345$	108.32	105.10	104.08	107.92	102.33
	106.72	104.08	104.60	107.91	103.30
	108.25	105.11	103.83	108.21	107.01
$\angle 456$	108.31	103.09	104.59	105.11	102.33
	108.24	105.48	104.60	105.53	104.20
	108.86	105.11	104.78	104.15	105.41
$\angle 623$	110.02	113.13	—	111.02	110.61
	109.95	113.28	106.51	111.35	110.57
	110.56	113.53	107.18	111.05	111.09
$\angle 562$	106.67	108.34	111.85	103.78	110.73
	106.49	108.35	112.07	102.86	110.8
	105.54	108.39	112.92	104.15	103.8
T_{5432}	0.00	0.03	0.00	0.00	0.11
	−12.60	−4.53	−2.20	−0.44	1.00
	−0.06	−0.06	−1.00	2.11	−2.20
T_{6543}	0.02	−0.08	0.00	0.00	−0.11
	−14.04	4.26	0.016	0.57	−0.92
	−0.89	1.96	0.05	−3.17	+2.30
ΔH_f/kcal	−57.11	−59.29	−92.99	−94.03	−128.92
	−59.43	−62.15	−97.25	−97.47	−132.79
	−59.97	−62.58	−96.99	−96.99	−97.51

Table 5. MNDO geometries for di-, tri-, and tetra-substituted 2-oxo-1,3-dioxolanes.

	t((**2a**) *c*-(**2a**) *g*-(**2a**)	*t*(**2c**) *c*(**2c**) *g*(**2c**)	*t*-(**2d**) *c*-(**2d**) *g*-(**2d**)	*t*-(**2e**) *c*-(**2e**) *g*-(**2e**)	*t*-(**2b**) *c*-(**2b**) *g*-(**2b**)	*t*-(**2f**) (**3**) (**4**)
C(2)–O(1)	1.216	1.211	1.209	1.211	1.215	1.212
	1.216	1.211	—	1.211	1.215	1.216
	1.216	1.211	1.210	1.211	1.215	1.217
C(2)–O(3)	1.367	1.376	1.376	1.373	1.368	1.374
	1.366	1.375	—	1.371	1.366	1.365
	1.366	1.382	1.385	1.381	1.369	1.362
O(3)–C(4)	1.418	1.399	1.404	1.410	1.420	1.408
	1.419	1.402	—	1.413	1.423	1.419
	1.426	1.393	1.400	1.412	1.425	1.425
C(4)–C(5)	1.589	1.582	1.591	1.600	1.609	1.588
	1.591	1.585	—	1.610	1.613	1.590
	1.591	1.584	1.600	1.611	1.605	1.630
C(5)–O(6)	1.418	1.399	1.404	1.410	1.420	1.409
	1.419	1.402	—	1.411	1.418	1.417
	1.411	1.413	1.409	1.409	1.413	1.425
O(6)–C(2)	1.367	1.376	1.375	1.372	1.368	1.371
	1.366	1.366	—	1.370	1.370	1.365
	1.368	1.368	1.366	1.366	1.367	1.362
∠123	124.70	125.13	125.25	125.16	124.74	124.72
	124.73	125.14	—	125.27	124.90	124.73
	124.74	124.34	124.21	124.23	124.40	124.77
∠234	111.24	111.21	111.75	111.85	111.66	111.49
	111.37	111.38	—	112.32	111.50	111.97
	111.66	111.12	111.90	112.24	111.16	111.44
∠345	103.43	103.77	103.39	103.39	102.94	103.50
	103.35	103.67	—	101.74	103.00	102.52
	102.37	104.38	103.24	102.30	103.17	102.33
∠456	103.43	103.72	103.50	103.09	102.95	103.57
	103.35	103.67	—	102.90	102.82	103.50
	104.43	103.18	103.37	103.85	103.11	102.32
∠623	110.61	109.73	109.50	109.70	110.55	109.91
	110.53	109.70	—	109.42	110.63	110.55
	110.60	109.95	109.53	109.91	110.64	110.47
∠562	111.24	111.21	111.75	—	111.60	111.51
	111.37	111.3	—	111.62	111.83	111.50
	110.93	113.70	111.92	111.70	111.88	111.44
T_{5432}	1.51	5.26	0.33	5.41	4.17	−0.76
	−0.50	2.58	—	11.57	4.80	−2.48
	0.00	0.17	0.05	−0.08	2.02	0.11
T_{6543}	−1.79	−6.27	−0.39	−6.29	−4.90	0.99
	0.00	0.03	—	−13.90	−4.14	3.28
	0.00	−0.24	−0.09	0.16	−1.53	−0.12
ΔH_f/kcal	−136.36	−138.02	−410.46	−140.15	−212.08	−312.04
	−134.90	−135.08	—	−129.88	−207.99	−134.16
	−133.13	−133.43	−402.67	−123.56	−210.10	−128.92

additional forces on the ring, non-planar conformations and ring-conformer interconversions of 1,3-dioxolanes[10a] and 4-butyrolactones[18–20] are well recognized.

Recently, crystallographic data of 1,3-dioxolanes[21,22] have demonstrated a twist angle in the range T_{3456} = 28–37°. *ab initio* molecular-orbital (MO) calculations (4-31G basis set) for 1,3-dioxolane showed an energy difference of 1.4 kcal between the planar (least stable) and the C_2 conformer.[10b] For 4-butyrolactone[18] the energy difference between conformers is again *ca.* 0–1.3 kcal.

In contrast with the above results the MNDO calculations presented here predict the planar conformation as the most stable form. However it is possible from these calculations to evaluate the tendency of a five-membered ring system to undergo ring deformation.

Table 7 presents the ΔH_f values of five-membered ring systems and their monomethyl derivatives at different T_{3456} angles (cyclopentanones (**5**)–(**5b**), oxolanes (**6**)–(**6b**), 1,3-dioxolanes (**7**)–(**7b**), 4-butyrolactones (**8**)–(**8c**) and 2-oxo-1,3-dioxolanes [(**1**), (**1a**)]. It appears that cyclopentanone possesses the greatest tendency for deformation. The energy barrier between the planar form and C_2 at T_{3456} = 20° is *ca.* 0–0.2 kcal in the monomethyl derivatives and 0.4 kcal in cyclopentanone. A further increase in the torsional angle to 30° increases the energy barrier ($\Delta\Delta H_f$) to 0.95, 0.56, and 1.35 kcal for (**5b**), (**5a**), and (**5**), respectively. According to the Boltzman weighting equation[24] a 1 kcal difference decreases the population of the less stable conformer to *ca.* 15%. The calculations indicate that among the substituted compounds: (*a*) two enantiomeric structures with opposite distortion (negative and positive torsional

Table 6. Geometric parameters of substituted 2-oxo-1,3-dioxolanes produced from MNDO calculations. Crystallographic data are according to the following notation.

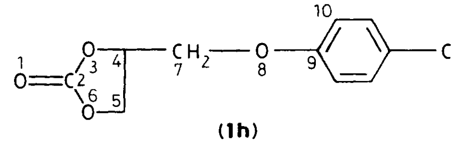

(1h)

	(1d) **(1i)**	**(1e)** **(1k)**	**(1b)** **(1j)**	**(1f)** **(1l)**	**(1g)** **(1c)**	 **(1m)**	**(1h)**[a] (MNDO) **(1h)** (crystallogs)[b]
C(2)–O(1)	1.216 1.215	1.215 1.215	1.215 1.213	1.216 1.210	1.216 1.213	— 1.213	1.215 1.192(6)
C(2)–O(3)	1.369 1.372	1.371 1.372	1.368 1.375	1.368 1.384	1.368 1.377	— 1.375	1.369 1.316(6)
O(3)–C(4)	1.416 1.413	1.418 1.414	1.422 1.411	1.417 1.406	1.420 1.399	— 1.412	1.417 1.443(5)
C(4)–C(5)	1.577 1.577	1.578 1.577	1.586 1.588	1.576 1.588	1.581 1.573	— 1.589	1.578 1.498(7)
C(5)–O(6)	1.412 1.411	1.413 1.412	1.412 1.412	1.412 1.410	1.412 1.413	— 1.411	1.412 1.420(6)
O(6)–C(2)	1.368 1.368	1.367 1.369	1.369 1.365	1.368 1.365	1.369 1.369	— 1.369	1.569 1.316(6)
∠123	124.63 124.55	124.50 124.63	124.77 124.60	124.64 123.66	124.71 124.55	— 124.62	124.74 124.6(4)
∠234	111.06 111.08	111.23 111.09	111.10 111.16	111.16 111.64	111.10 110.96	— 111.07	115.15 109.7(4)
∠345	103.47 103.56	103.23 103.54	103.25 103.64	103.30 103.24	103.24 104.21	— 103.57	103.35 103.7(4)
∠456	104.06 103.98	104.13 104.02	103.76 103.40	104.20 103.85	104.13 103.62	— 103.47	104.15 103.8(4)
∠623	110.53 110.38	110.39 110.39	110.50 110.14	110.57 109.67	110.65 110.09	— 110.25	110.52 111.9(4)
∠562	110.87 110.99	110.99 110.95	111.27 111.52	110.75 111.57	110.84 110.97	— 111.40	110.85 110.8(4)
T_{5432}	1.180 0.366	—0.58 −0.62	3.67 3.57	0.81 −1.39	−1.82 3.88	— 4.77	−0.34 2.0(5)
T_{6543}	−0.68 −0.20	0.76 0.61	−2.92 −3.02	−0.35 0.75	1.77 −3.00	— −3.93	0.14 −3.4(5)
ΔH_f	−169.66 −323.59	−139.35 −174.63	−170.04 −322.99	−119.44 −71.75	−98.00 −133.79	 −179.65	−142.93

[a] $R_{47} = 1.565\ (1.534)$; $R_{78} = 1.404\ (1.431)$; $R_{89} = 1.3712\ (1.381)$; $\theta_{743} = 111.5\ [108.5(4)]$; $\theta_{874} = 109.1\ [108.6(4)]$; $\theta_{987} = 119.9\ (115.6)$; $T_{7432} = -124.1\ [-121.7(4)]$; $T_{8743} = -70.9\ [65.0(4)]$; $T_{9874} = 144.3\ [-169.1(3)]$; $T_{10987} = -106[176.9(3)]$. [b] Estimated standard deviations are in parentheses.

angles) do not exhibit equal energy. The preferred form in general corresponds to a positive value where the methyl group adopts a quasi-equatorial conformation, and (*b*) ring substitution by a methyl group decreases (at least for one of the enantiomers) the interconversion energy barrier (except for ethylene carbonate).

In the case of oxolanes (**6a**, **b**) and 4-butyrolactones (**8a**–**c**), the energy barrier between the planar and the stable conformer at 20° distorsion is less than 1 kcal. This difference permits a significant amount of the C_2 conformers to exist. In the case of 1,3-dioxolanes and 2-oxo-1,3-dioxolanes, the respective barriers have higher enthalpy values. It seems therefore that in comparison with other five-membered ring systems the presence of two endocyclic oxygens, restricts ring puckering. The energy barriers order in the planar $\longleftrightarrow$ twist interconversion in the above ring systems is carbonates > 1,3-dioxolanes > butyrolactones > oxolanes > cyclopentanones.

Crystallographic data of non-substituted 2-oxo-1,3-dioxolane and of the compound substituted with strong electron-withdrawing groups such as 4,5-bis-fluorodinitromethyl[23] show a non-planar structure with $T_{3456} = 28–31°$. In contrast with these results the crystal structure of 4-chlorophenyloxymethyl-1,3-dioxolan-2-one (1h) displayed a virtually planar conformation. Values of geometric parameters from crystal-structure and MNDO calculations are given in Table 6.

In general there is a good correlation between the computed and the measured bond lengths, bond angles, and dihedral angles. However, several differences were observed: (*a*) the backbone conformation according to computation is planar while a ring deformation of −3.40(5) is observed in the crystal structure; (*b*) the oxygen bond angles in the side chain differ by 4.2°; (*c*) the oxygen torsional angle T_{8743} according to MNDO calculations is −70.9°, however, from the crystal data the corresponding value is +65.0° (4); (*d*) the phenyl ring in the crystal deviates by 3.1(3)° from the plane of atoms 7–8–9 while the computed value yields a rotation of 74°. In addition some differences in *R*[C(4)–C(5)] and θ(2, 3, 4) are also found.

MNDO conformational-energy calculations of (**1**), (**1a**), and (**1h**) show a preference for a planar conformation. In order to assess the contributions of electronic and steric effects we

Table 7. ΔH_f values of cyclopentanones, oxolanes, 1,3-dioxolanes, 4-butyrolactones, and 2-oxo-1,3-dioxones at various values of T_{3456}.

	ΔH_f/kcal			
Compound	T_{3456} 0° 0°	T_{3456} +10° −10°	T_{3456} +20° −20°	T_{3456} +30° −30°
(5)	−57.11	−57.04 −57.04	−56.70 −56.70	−55.76 −55.76
(5b)	−59.96	−59.95 −59.89	−59.76 −59.61	−59.01 −58.73
(5a)	−59.28	−59.11 −59.11	−59.35 −58.78	−58.72 −57.88
(6)	−59.29	−59.07 −59.07	−58.29 −58.29	−56.53 −56.53
(6b)	−62.58	−62.46 −62.31	−61.83 −61.49	−60.26 −59.67
(6a)	−62.13	−62.10 −61.84	−61.58 −61.07	−60.13 −59.32
(7)	−93.00	−92.69 −92.69	−91.64 −91.64	−89.52 −89.52
(7a)	−97.25	−96.95 −96.95	−95.91 −94.60	−93.80 −92.51
(7b)	−96.90	−96.70 −96.53	−95.82 −95.45	−93.90 −93.20
(8)	−94.03	−93.79 −93.79	−92.95 −92.96	−91.21 −91.21
(8a)	−97.47	−97.28 −97.22	−96.56 −96.43	−94.99 −94.71
(8b)	−96.97	−96.66 −96.90	−95.87 −96.33	−94.22 −94.88
(8c)	−97.50	−97.38 −97.17	−96.71 −96.26	−95.17 −94.36
(1)	−45.93	−45.77 −45.77	−44.91 −44.91	−42.90 −43.55
(1a)	−132.79	−132.30 −132.32	−131.22 −130.90	−128.72 −128.15

Table 8. Values of T_{endo} and T_{exo} as calculated by MNDO of various mono-substituted 2-oxo-1,3-dioxolanes.

R	T_{endo}	T_{exo}
CH_2OMe	−126.2	60.7
CH_2OCF_3	−127.3	60.2
$CH_2OC_6H_4Cl$	−124.1	−70.9
CH_2F	−127.7	58.1
CH_2Cl	−127.3	180
Cl	−117.0	—
OCH_3	−113	−79
OCF_3	−112.7	−62.8
$OCCl_3$	−112.2	−99.4
Me	−126.4	—

extended the calculations to various types of polar substituents and to polymethyl substituents. The results are presented in Tables 5 and 6. It can be seen that with respect to *c*-(**2a**), *t*-(**2a**), and *g*-(**2a**) dimethyl substituents, only the *trans* isomer experiences slightly increased ring distortion (T_{3456} = 1.80°). With dichlorosubstituents *t*-(**2c**), *c*-(**2c**), and *g*-(**2c**) the *trans* isomer again experienced the most ring deformation ($T_{3456} = -6.30$). However, with OCH_3 (*t*-(**2b**) and *c*-(**2b**) both *cis* and *trans* isomers exhibited a small degree of ring puckering. CF_3 did not exert any significant effect on the planar form, although a bulky substituent such as CCl_3 appears to bring about considerable conformational changes.

Steric hindrance and polar repulsive interactions between these substituents in the *cis* position *c*-(**2e**) imposes a relatively high degree of ring distortion (T_{3456} = 13.6°). The *trans* isomer *t*-(**2e**) experiences a moderate effect similar to that felt by Cl *t*-(**2c**) (T_{3456} = 6.3°). In all cases the effect of *gem*-dialkyl groups on the ring conformation was negligible.

Comparison between the torsional angles (Tables 5, 6) in mono- and di-substituted carbonates [(**1c**), *t*-(**2c**); (**1b**), *t*-(**2b**)] suggests that substituent effect on T_{3456} is additive [3° *vs.* 6.2° and 2.9° *vs.* 4.9° in (**1c**), *t*-(**2c**), and (**1b**), *t*-(**2b**), respectively].

The T_{3456} value of the 2,2,3-trimethyl derivative of ethylene carbonate (**3**) and the 2,2,3,3-tetramethyl derivative of ethylene carbonate (**4**) is close to zero. Since puckering of the latter compound does not seem to relieve steric strain, the data indicates that the reduction of strain occurs *via* the increase in R_{45} bond length up to 1.630 Å.

The 'anomeric effect' is a well recognized phenomenon[25,26] related to the tendency of electronegative substituents at anomeric carbon in pyranose rings to prefer an axial position to an equatorial one. It was first interpreted in terms of dipole–dipole interaction and latter by the $n \longrightarrow \sigma^*$ electron donation from oxygen lone pair to the antibonding C–O orbital of an adjacent C–O bond.

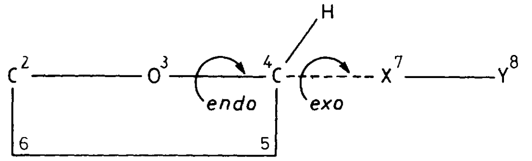

This type of stabilization is expected to lead to a preference for a *gauche* conformation for atoms 2, 3, 4, 5 (T_{endo} *ca.* 60°). If X = O (or any other electronegative atom) an *exo* anomeric effect in atoms 3, 4, 7, 8 is also expected (T_{exo} *ca.* 60°).

The more electronegative the X substituent is, the lower the corresponding σ^* (C–X) orbital (*i.e.* an increase in acceptor properties). Lowering of the σ^* orbital can also be achieved by increasing the electronegativity of Y. On the other hand, an electron-donating substituent on C(2) is expected to increase the oxygen lone-pair orbital level and its donation properties. These two parameters seem to enhance the anomeric effect.

In cyclic carbonates, the carbonyl on C(2) reduces the availability of the n_p lone pair electrons on O(3) to overlap with orbitals of C(4). It is conceivable, however, that replacing X or Y by strong electron-withdrawing substituents will enhance conformational changes due to the anomeric effects.

Table 8 summarizes the torsion angles (T_{endo} and T_{exo}) for several cyclic carbonates substituted at C(4) with strong electron-withdrawing groups. From the data it is inferred that the ring is approximately planar and that group X adopts a bisecting position with T_{endo} 111–128°. In addition, almost all polar groups in Y are oriented in a *gauche* conformation (T_{exo} = 60–100°) except for Cl.

In 4,5-disubstituted ethylene carbonate T_{exo} for *trans*-4,5-dimethoxy groups are −82.2 and 81.9°. For the *cis* isomer the corresponding values are −85.7 and 31.2° and for the *gem*-dimethoxy isomers the T_{exo} values are 68.8 and 17.3°. These results indicate that when a disubstituted compound is sterically hindered, at least one of its alkoxy groups adopts a *gauche* conformation. It is also noteworthy (Table 8) that CH_2Cl and CH_2F do not display similar T_{exo} values in their optimized structures. Table 9 presents additional data calculated by MNDO for the rotation around C(4)–X(7) bond (T_{exo}). It appears that both ΔH_f and T_{endo} depend on T_{exo} values. The

Table 9. Rotamer effect on ΔH_f, torsional angles, dipole moments, and bond lengths in 2-oxo-1,3-dioxolanes, as derived from MNDO calculations.

T_{exo}		0°	30°	60°	90°	120°	150°	180°	210°	240°	270°	300°	330°
ΔH_f	CH_2Cl	135.0	136.7	138.4	137.3	135.9	137.4	139.4	138.6	137.3	137.9	138.0	136.2
	CH_2F	172.2	173.6	174.6	173.2	171.7	172.7	174.2	173.3	172.2	173.2	173.9	172.9
	CH_3O	166.8	166.9	166.7	165.5	163.9	163.9	165.6	167.4	168.7	169.9	169.7	168.0
T_{endo}	CH_2Cl	−126.6	−126.8	−128.2	−130.2	−131.8	−131.0	−127.3	−125.9	−125.9	−125.5	−125.1	−125.4
	CH_2F	−126.6	−126.8	−127.7	−129.4	−130.9	−130.1	−127.1	−125.8	−125.8	−125.6	−125.3	−125.6
	CH_3O	−121.1	−124.5	−126.5	−127.1	−124.8	−121.5	−118.1	−114.3	−113.1	−113.2	−114.7	−117.5
T_{2345}	CH_2Cl	−0.38	−0.78	−0.59	0.18	−1.32	−3.32	−1.69	−0.47	−0.98	−1.62	−0.77	−0.23
	CH_2F	−0.58	−1.02	−0.42	0.26	−1.00	−2.56	−1.55	−0.52	−1.07	−1.90	−1.22	−0.32
	CH_3O	0.65	0.14	0.97	1.88	3.54	4.09	3.92	4.51	4.39	3.88	3.20	2.14
μ	CH_2Cl	5.54	5.79	5.38	4.84	4.05	3.32	2.89	2.95	3.52	4.31	4.90	5.35
	CH_2F	5.68	5.69	5.44	4.88	4.12	3.39	2.95	2.99	3.56	4.33	5.02	5.47
	CH_3O	3.42	3.50	3.94	4.52	5.11	5.53	5.74	5.80	5.61	5.10	4.42	3.77
R_{43}	CH_2Cl	1.4138	1.4138	1.4150	1.4167	1.4182	1.4188	1.4185	1.4185	1.4181	1.4171	1.4116	1.4114
	CH_2F	1.4132	1.4133	1.4143	1.4156	1.4163	1.4163	1.4159	1.4161	1.4162	1.4158	1.4148	1.4138
	CH_3O	1.4173	1.4190	1.4227	1.4256	1.4246	1.4209	1.4180	1.4183	1.4211	1.4228	1.4215	1.4187

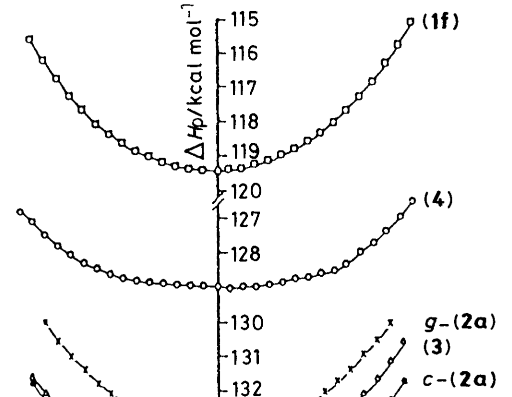

Figure 2. The effect of ring torsion (T_{3456}) in substituted ethylene carbonates on ΔH_f.

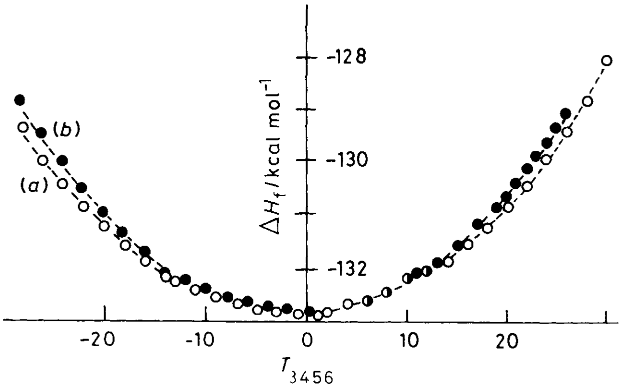

Figure 3. Energy barrier ΔH_f in (**1b**) due to changes on T_{3456}: (*a*) T_{3456} calculated with no constraints; (*b*) T_{3456} calculated under the constraint T_{1234} = 180°.

maximal changes in ΔH_f due to rotation around the C(3)–X(4) bond is 4.4, 2.9, and 6.0 kcal for CH_2Cl, CH_2F, and OCH_3, respectively. In the case of CH_2Cl and CH_2F, rotation of the polar groups Cl and F in O–C–C–X (X = Cl, F) from the eclipsed conformation (T_{exo} = 0) to higher dihedral angles gives rise to a constant increase in T_{endo} up to a maximum of T_{exo} = 120–150°. A further rotation decreases T_{endo} values. Ring puckering (T_{2345}) increases accordingly with a maximal value at T_{exo} = 150°.

It is also noticeable that (*a*) the conformation of the molecule related to the maximum does not coincide with the most stable form which occurs at T_{exo} = 58.1 and 180° for F and Cl, respectively and (*b*) the trend in T_{exo} is not reflected by the total change in dipole moment. On the other hand, T_{endo} seems to correlate with the R_{34} bond length. The increase of puckering toward a pseudo-axial position of a substituent is accompanied by a lengthening of the R_{34} bond. Although the displayed correlation deals with small effects, the tendency of this relationship is not in accordance with the anomeric effect where an O–CH_2 bond in C–O–CH_2CH_2X is expected to shorten.

In the case where X–Y in C(2)–O(3)–C(4)–X(7)–Y(8) is OCH_3, T_{exo} operates in an opposite direction. An increase in T_{exo} decreases T_{endo} until a minimum is reached at T_{exo} = −90° (for T_{2345} the minimum is at −150°). This is probably due to the opposite direction of the C–O–C dipole moment vector compared with that of CH_2–X at any torsional angle. In this case the conformation of the molecule at the minimum is very close to the most stable conformation. However in contrast with the above, the tendency of ring puckering is toward a quasi-equatorial substituent position rather than a quasi-axial position. Since the R_{43} bond length values are scattered, no correlation can be made.

From these models (CH_2X, CH_2OCH_3), it seems that steric factors might also be operative and have to be taken into consideration. In general it can be said that the role of the anomeric effect in ring puckering of ethylene carbonate is small. The potential barriers of ring puckering *via* variation of torsional angles T_{3456} are given in Table 8 and in Figure 2.

From the data it is inferred that the potential curves incline moderately and for most of the compounds a 1 kcal difference between $^4T_5$ or $^5T_4$ conformers and the planar form corresponds to a torsional angle of ±14–16°. In the case of (**4**) (tetramethyl derivative) the minimum is less curved and a torsional angle of ±20° increases ΔH_f by only 0.63 kcal.

By analogy with (**1a**), $^4T_5$ conformers in (**1e**), (**1f**), and (**1h**) are more stable than their $^5T_4$ enantiomers (the substituents are in quasi-equatorial orientations). However, in the case of (**1d**), $^5T_4$ is the most stable one. It was also noted that with dimethyl substituents [*t*-, *c*-, and *g*-(**2a**)] the *gem*-dialkyl isomer *g*-(**2a**) is more resistant to ring torsion than the *trans*- or the cis-(**2a**) isomers.

The energy barriers of the compounds (**2a**) are identical and no preference for either $^4T_5$ or $^5T_4$ conformers was observed. In addition to $^4T_5$ and $^5T_4$ conformers, we considerd some additional modes. Figure 3 presents energy barriers (ΔH_f) for two modes of variable dihedral angles of (**1a**). Case (*a*) corresponds to the change of T_{3456} with no constraints on other backbone dihedral angles. Case (*b*) refers to T_{3456} twisted angles with T_{1234} fixed at 180°. The latter allows the formation of slightly deformed ^5E and E_5 conformers, in which O(6) is out of the O–C–O plane in the direction of C(5) with $q(6)$=0.15$q(5)$ (q is the displacement in the *z* direction, and corresponds to the puckering amplitude in a pseudorotation circuit). It can be seen (Figure 3) that the twisted form of case (*a*) is slightly more stable than that of case (*b*), particularly at high degrees of puckering.

Other types of ring puckering were obtained according to the following operations (Figure 4): (*a*) case (*c*), twisting about the C(5)–C(6) bond (T_{2654}), (*b*) case (*i*), twisting of C(3)–C(4) bond (T_{2345}), (*c*) case (*b*), twisting at the C(3)–C(4) bond with T_{1234} fixed at 180°, (*d*) case (*j*), twisting at the C(5)–C(6) bond with T_{1265} = 180°, and (*e*) case (*f*), twisting at the C(3)–C(4) bond with T_{3456} = 0°. Cases (*c*) and (*i*) result in slightly deformed (^5E, E_5) and (^4E, E_4) envelope forms, respectively, while case (*f*)

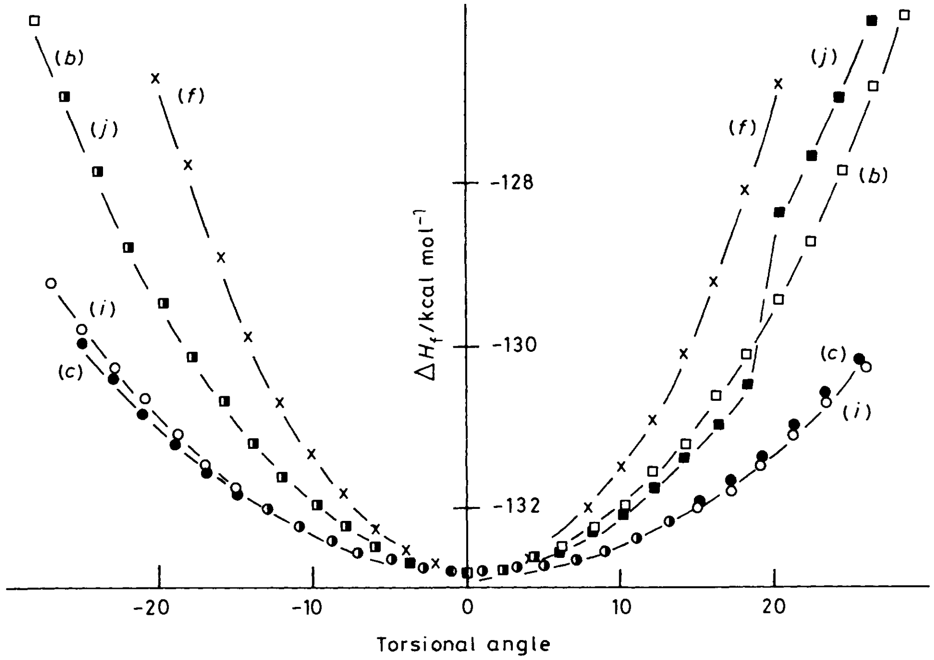

Figure 4. The effect of various modes of twisted angle (T) in IB on ΔH_f. (c) T_{4562}; (i) T_{2345}; (b): T_{2345} while T_{1234} = 180°; (j) T_{4562} while T_{1265} = 180°; (f) T_{2345} while T_{3456} = 0°.

Table 10. ΔH_f values of substituted cyclic carbonates and iminocarbonates of planar and twisted forms.

	ΔH_f/kcal			
T_{3456} Comp.	0°	+10° −10°	+20° −20°	+30° −30°
t-(**2a**)	−136.55	−136.30 −136.30	−135.16 −135.16	−132.78 −132.78
c-(**2a**)	−134.90	−134.59 −134.59	−133.49 −133.49	−131.19 −131.19
g-(**2a**)	−133.13	−132.74 −132.74	−131.43 −131.43	−128.78 −128.78
(**3**)	−134.13	−133.66	−132.45	130.00
(**4**)	−128.92	−128.83 −128.83	−128.29 −128.29	−126.59 −126.59
(**1d**)	−169.66	−169.15 −169.27	−167.78 −167.85	−165.15 −164.94
(**1e**)	−134.40	−138.04 −137.89	−136.74 −136.30	−134.18 −133.27
(**1f**)	−119.44	−119.02 −119.06	−117.74 −117.70	−115.17 −114.92
(**1h**)	−142.93	−142.60 −142.46	−141.35 −141.03	−138.85 −138.25
Z-(**1a**)	−48.90	−48.57 −48.42	−47.44 −47.11	−45.10 −44.50
E-(**1a**)	−48.89	−48.59 −48.45	−47.44 −47.13	−45.10 −44.55
Z-(**1g**)	−14.04	−13.49	−12.00	9.87(28°)

corresponds to the (^2E, E_2) form. Case (b) results in a significantly deformed envelope conformation where C(2), O(3), and C(4) residue in the same plane while C(5) and O(6) are out of plane in the same direction. The displacement of O(6) is *ca.* 0.45 of qC(5). Case (j) resembles 2A with C(2), O(6), and C(5) in plane. The displacement of O(3) in the z direction is $q3 = 0.45q4$. It can be seen that the energy barrier in ^5E, E_5 ^4E, E_4 [cases, (c) and (i)] conformers is lower than in the other envelope forms. A change of *ca.* 13° in T_{2654} [case (c)] or in T_{2345} [case (i)] corresponds to *ca.* 0.6 kcal only.

The present study also includes calculations on some iminocarbonates *Z*- and *E*-(**1a**) and *Z*-(**1g**). From Table 10 it is deduced that five-membered ring cyclic carbonates and five-membered ring iminocarbonates have similar energy barriers to conformer interconversions. By analogy with the monosubstituted carbonates twisting of the iminocarbonates by T_{3456} = 14–16° gives rise to H_f of *ca.* 1 kcal. No significant difference between the *E* and *Z* conformers was observed. In the planar conformation the phenyl group rotates out of the O–C–O plane of *Z*-(**1a**) and *Z*-(**1g**) by 82.1 and 78.7°, respectively.

Experimental

N.M.R Spectroscopy.—Samples for N.M.R. measurement were dissolved in $CDCl_3$ and examined at 20 °C on a Bruker 200 MHz spectrometer. ^{13}C spectra were examined with broadband decoupling of the ^1H region. For ^{13}C coupling constants studies, gated ^1H decoupling was employed. When ^3J coupling, of the $^{13}C{=}O$ by the cyclic carbonate ring protons, was studied, narrow spectrum widths were examined to achieve a computer resolution better than 0.2 Hz per point.

Heat of Formation (ΔH_f).—Semiempirical SCF calculations were carried out using MNDO.[27] Total geometry optimization, including internal rotations, was applied to each of the molecular species. Second derivatives were estimated for all $3N - 6$ geometrical parameters during optimization. The minima were verified through the second derivatives (Hessian) matrix eigenvalues, which must be all positive.

DFP[28] analytical gradients were used throughout the optimization. Entropies were calculated by evaluation of the vibrational, rotational, and translational partition functions.[29] As small differences were found between the entropies in each transformation scheme, these values are not reported.

Table 11. Experimental details of the *X*-ray diffraction studies of 4-chlorophenoxymethyl-1,3-dioxolan-2-one.

Formula	$C_{10}H_9O_4Cl$
a/Å	16.042(2)
b/Å	5.374(1)
c/Å	11.535(2)
β/°	92.36(1)
V/Å^3	993(1)
M_F	228.5
Z	4
D_{calc}	1.53
Space group	$P2_1/c$
Min. obs. coeff/cm^{-1} [a]	32.18
No. of unique data	1 434
No. of obs unique data [b]	1 305
No. of parameters refined	138
Max. parameter shift in final refinement cycle	0.05
Max. electron density on final difference Fourier map	0.438
$R1$ [c]	0.0530
$R2$ [d]	0.0525

[a] No absorption correction was applied. [b] $F_0 > 3\sigma(F_0)$. [c] $R1 = \Sigma||F_o| - |F_c||/\Sigma|F_o|$. [d] $R2 = [\Sigma w(|F_o| - |F_c|)^2/\Sigma w|F_o|^2]^{\frac{1}{2}}$.

Table 12. Positional parameters and estimated standard deviations for (**1h**).

Atom	x	y	z
Cl	0.454 65(7)	0.116 3(2)	0.165 5(1)
O(1)	0.050 1(2)	0.896 6(8)	−0.321 6(3)
C(2)	0.077 9(3)	1.010 9(9)	−0.240 2(4)
O(3)	0.065 9(2)	0.954 4(5)	−0.131 1(3)
C(4)	0.109 0(3)	1.131 3(9)	−0.056 0(4)
C(5)	0.146 6(3)	1.310 3(9)	−0.138 5(4)
O(6)	0.125 5(2)	1.208 7(7)	−0.249 5(3)
C(7)	0.170 8(3)	0.989 2(9)	0.024 5(4)
O(8)	0.233 1(2)	0.878 7(5)	−0.044 5(2)
C(9)	0.284 9(2)	0.708 6(8)	0.012 0(3)
C(10)	0.280 7(2)	0.650 0(8)	0.128 9(3)
C(11)	0.333 9(3)	0.466 5(8)	0.174 3(3)
C(12)	0.390 1(2)	0.347 9(7)	0.105 5(3)
C(13)	0.395 4(2)	0.411 5(8)	−0.009 2(3)
C(14)	0.342 5(2)	0.592 3(8)	−0.056 1(3)

[a] Estimated standard deviations in the least significant digits are shown in parentheses.

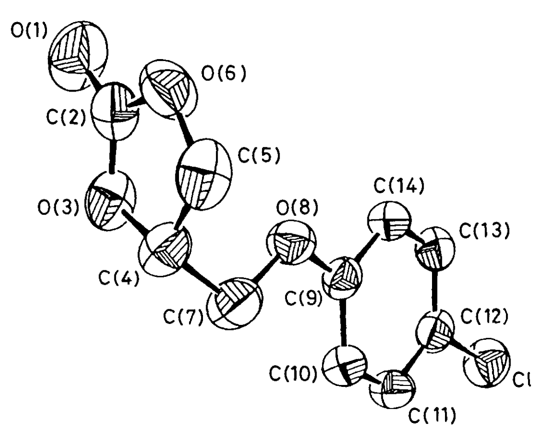

Figure 5. Structure of (**1h**) showing the 50% probability thermal ellipsoids and atom-labelling scheme.

Crystallizations.—*X*-Ray quality crystals were obtained by recrystallization of (**1h**) from a mixture of light petroleum–diethyl ether and ether.

Data Collection and Processing.—The crystals were glued onto glass fibre using epoxy resin. The data were collected on an Enraf–Nonius CAD-4F automated diffractometer with monochromatised Cu-K_α (λ = 1.5418 Å) radiation. Unit-cell parameters were obtained by a least-squares fit of 20 high-angle reflections. The crystal system was found to be monoclinic and the space group was determined to be $P2_1/c$ ($C_{2s}{}^5$, No. 14)[30] from the systematic absences and, ultimately, from the solution and successful refinement of the structure. The data were collected in the θ–2θ scan mode. Lorentz and polarization corrections were applied. The intensities of the 3 standard reflections did not exhibit any decay and no correction was applied. No absorption correction was applied. Other information pertinent to data collection and processing is given in Table 11.

Structure Analysis and Refinement.—The solution to the structure was obtained with the aid of the direct methods program MULTAN.[31] The atomic positions of the chlorine and oxygen atoms were introduced and refined and the positions of the remaining non-hydrogen atoms were obtained from subsequent refinements and difference Fourier Maps.

Anisotropic thermal parameters were used for the chlorine, oxygen and carbon atoms. The hydrogen atoms were constrained to 'ride' on the carbon atoms and the aromatic hydrogens were refined with a common thermal parameter as were the aliphatic hydrogen atoms.

Using SHELX-76,[32] full-matrix least-squares refinements were carried out. Using unit weights, the refinement converged to satisfactory discrepancy indices which are listed in Table 11.

Final non-hydrogen positional parameters, together with their estimated standard deviations appear in Table 12. Selected interatomic distances, bond angles, and torsion angles, together with their standard deviations appear in Table 6. Figure 5 depicts the molecular geometry and labelling scheme for 4-chlorophenyloxymethyl-1,3-dioxolan-2-one. The thermal parameter of the non-hydrogen atoms and the positional and thermal parameters of the hydrogen atoms have been deposited at the Cambridge Crystallographic Data Centre.*

References

1 (*a*) K. S. Pitzer, *Science*, 1945, **101**, 672; (*b*) J. E. Kilpatrick, K. S. Pitzer, and R. Spitzer, *J. Am. Chem. Soc.*, 1947, **69**, 2483; (*c*) *ibid*, 1958, **80**, 6697; (*d*) K. S. Pitzer and N. E. Donath, *J. Am. Chem. Soc.*, 1959, **81**, 3213.
2 (*a*) C. Altona, H. J. Geise, and C. Romers, *Tetrahedron*, 1968, **24**, 13; (*b*) C. Altona, *Pure Appl. Chem.*, 1971, **25**, 1.
3 J. B. Lambert, J. J. Papay, S. A. Khan, K. A. Kappauf, and E. S. Magyar, *J. Am. Chem. Soc.*, 1974, **96**, 6112.
4 T. M. Filippova, B. D. Laurukhin, I. K. Shmyrev, *Org. Magn. Reson.*, 1974, **6**, 92.
5 B. Fuchs and P. S. Wechsler, *Tetrahedron*, 1979, **33**, 57.
6 C. Altona, H. R. Buys, and E. Havinga, *Recl. Trav. Chim. Pays-Bas*, 1966, **85**, 973.
7 C. Romers, C. Altona, H. R. Buys, and E. Havinga, *Top. Stereochem.*, 1969, **4**, 39.
8 (*a*) N. L. Allinger, J. A. Hirsch, M. A. Miller, I. J. Tyminski, F. A. van Catledge, *J. Am. Chem. Soc.*, 1968, **90**, 1199 (1968); (*b*) N. L. Allinger, M. T. Tribble, M. A. Miller, and D. A. Wertz, *ibid.*, 1971, **93**, 1637.
9 D. Cremer, J. S. Binkley, and J. A. Pople, *J. Am. Chem. Soc.*, 1976, **98**, 6836.
10 (*a*) C. Cremer and J. A. Pople, *J. Am. Chem. Soc.*, 1975, **97**, 1354; (*b*) *ibid.*, 1975, **97**, 1375.
11 (*a*) H. Kim and W. D. Gwinn, *J. Chem. Phys.*, 1969, **51**, 1815; (*b*) T. Iked and R. C. Lord, *ibid.*, 1969, **51**, 3225; (*c*) K. Tamagawa, R. L. Hilderbrandt, and A. Shens, *J. Am. Chem. Soc.*, 1987, **109**, 1380.

---

* For details of the CCDC deposition scheme, see 'Instructions for Authors' (1989), *J. Chem. Soc., Perkin Trans. 2*, 1989, Issue 1.

12 C. J. Brown, *Acta Crystallogr.*, 1954, **7**, 92.

13 (*a*) I. Ringel, J. Katzhendler, and A. Goldblum, submitted for publication; (*b*) K. Pihlaya and K. Rossi, Acta Chem. Scand., *Ser. B*, 1977, **31**, 899; *ibid.*, 1983, **37**, 289.

14 K. Tamagawa, R. L. Hilderblat, and A. Shen, *J. Am. Chem. Soc.*, 1987, **109**, 1380.

15 A. S. Serianni and A. Barker, *J. Org. Chem. 1984*, **49**, 3292.

16 C. Altona and M. Sundaralingam, *J. Am. Chem. Soc.*, 1972, **94**, 8205.

17 A. S. Serianni and D. M. Chipman, *J. Am. Chem. Soc.*, 1987, **109**, 5297.

18 T. Angelotti, M, Krisko, t. O'Connor, and A. S. Serionni, *J. Am. Chem. Soc.*, 1987, **109**, 4464.

19 N. V. Riggs, *Aust. J. Chem.*, 1985, **38**, 1575.

20 N. L. Allinger and S. H. M. Chang, *Tetrahedron*, 1977, **33**, 1561.

21 D. J. Chadwick and J. D. Dunitz, *Acta Crystallogr., Sect. B*, 1978, **34**, 965.

22 R. Bardi, A. M. Piazzesi, A. Del Pma, and L. Villa, *Acta Crystallogr., Sect. C*, 1983, **39**, 505.

23 H. L. Ammon and S. K. Bhattacharjee, *Acta Crystallogr., Sect. C*, 1984, **40**, 487.

24 L. Piela, G. Nemethy, and H. A. Scheraga, *J. Am. Chem. Soc.*, 1987, **109**, 4477.

25 A. Cosse-Barbi and J. E. Dubais, *J. Am. Chem. Soc.*, 1987, **109**, 1503 and references cited therein.

26 P. Aped, Y. Apeloig, A. Ellencweig, B. Fuchs, I. Goldberg, M. Karni, and E. Tartakovsky, *J. Am. Chem. Soc.*, 1987, **109**, 1486 and references cited therein.

27 M. J. S. Deward and W. Thiel, *J. Am. Chem. Soc.*, 1977, **99**, 4899.

28 R. Fletcher, *Comput. J.*, 1970, **13**, 317.

29 M. C. Flanigan, A. Komornicki, and J. W. McIven, in 'Semiempirical Methods of Electronic Structure Calculations,' ed. G. A. Segal, Plenum Press, N.Y., 1977, vol. 8, p. 1.

30 'International Tables for Crystallography,' ed. T. Hahn, D. Reidel Publishing Co., Dordrecht, Holland, 1983, vol. A, pp. 484–485.

31 P. Main, S. E. Hull, L. Lessinger, G. Germain, J. P. Declercq, and M. M. Woolfson, MULTAN 78, York, England, 1978.

32 G. M. Sheldrick, SHELX-76 in 'Computing in Crystallography,' eds. H. Schenck, R. Olthof-Hazekamp, H. van Koningsveld, and G. C. Bassi, Delft University Press, Delft, The Netherlands, 1978, pp. 34–42.

Received 25*th February* 1988; *Paper* 8/00746B